Available online at www.sciencedirect.com
ScienceDirect
Journal of Power Sources 176 (2008) 312–319
JOURNAL OF POWER SOURCES
www.elsevier.com/locate/jpowsour

Performance of Na_2O promoted alumina as CO_2 chemisorbent in sorption-enhanced reaction process for simultaneous production of fuel-cell grade H_2 and compressed CO_2 from synthesis gas

Ki Bong Lee, Michael G. Beaver, Hugo S. Caram, Shivaji Sircar *

Department of Chemical Engineering, Lehigh University, Bethlehem, PA 18015, USA

Received 18 August 2007; received in revised form 9 October 2007; accepted 9 October 2007
Available online 23 October 2007

Abstract

The performance of a novel thermal swing sorption-enhanced reaction (TSSER) concept for simultaneous production of fuel-cell grade hydrogen and compressed carbon dioxide as a by-product from a synthesis gas feed is simulated using Na_2O promoted alumina as a CO_2 chemisorbent in the process. The process simultaneously carries out the water gas shift (WGS) reaction and removal of CO_2 from the reaction zone by chemisorption in a single unit. Periodic regeneration of the chemisorbent is achieved by using the principles of thermal swing adsorption employing super-heated steam purge.

Recently measured equilibrium and kinetic data for chemisorption and desorption of CO_2 on the promoted alumina using conventional column dynamic tests as well as new experimental data demonstrating the concept of sorption-enhanced WGS reaction using the material are reviewed. The simulated performance of the TSSER process employing this material as a chemisorbent is compared with the process performance using K_2CO_3 promoted hydrotalcite as the chemisorbent. The promoted alumina exhibited (i) ∼15% lower H_2 productivity at a slightly reduced CO to H_2 conversion, and (ii) comparable compressed CO_2 productivity at a higher CO_2 recovery, albeit at a relatively lower product pressure. However, the steam duty for regeneration of the chemisorbent was reduced by ∼50% for the promoted alumina.

Keywords: Fuel-cell grade hydrogen; Carbon dioxide; Sorption-enhanced reaction; Thermal swing chemisorption; Promoted alumina; Promoted hydrotalcite

1. Introduction

A recent report prepared by the U.S. National Research Council and the National Academy of Engineering surmised that the vision of hydrogen economy is based on two expectations [1]:

- Hydrogen can be produced from domestic energy sources in a manner that is affordable and environmentally benign.
- Applications using hydrogen (e.g. fuel-cell vehicles) can get market share in competition with the alternatives.

One of the key R&D priorities is, therefore, to develop new ideas to produce fuel-cell grade H_2 from the synthesis gas generated by coal gasification, while capturing and recovering a pure CO_2 by-product. A novel cyclic thermal swing sorption-enhanced reaction (TSSER) process concept was recently proposed which can satisfy these goals [2]. It directly produces fuel-cell grade H_2 and compressed CO_2 as a by-product gas by reacting CO and H_2O from a synthesis gas produced by gasification of coal (after removal of trace sulfur impurities) in a single sorber-reactor packed with an admixture of a water gas shift (WGS) reaction catalyst and a CO_2 selective chemisorbent. The by-product CO_2 of the exothermic WGS reaction ($CO + H_2O \leftrightarrow CO_2 + H_2$; $\Delta H_R = -41\,kJ\,mol^{-1}$), which is thermodynamically controlled, is removed from the reaction zone to directly produce a fuel-cell grade H_2 from the sorber-reactor. The chemisorbed CO_2 is then periodically removed by super-heated steam purge using the principles of thermal swing adsorption so that the chemisorbent can be re-used. A part of the desorbed CO_2 is withdrawn as a compressed by-product gas by employing several complementary intermediate steps such as a CO_2

* Corresponding author. Tel.: +1 610 758 4469; fax: +1 610 758 5057.
E-mail address: sircar@aol.com (S. Sircar).

0378-7753/$ – see front matter © 2007 Elsevier B.V. All rights reserved.
doi:10.1016/j.jpowsour.2007.10.042

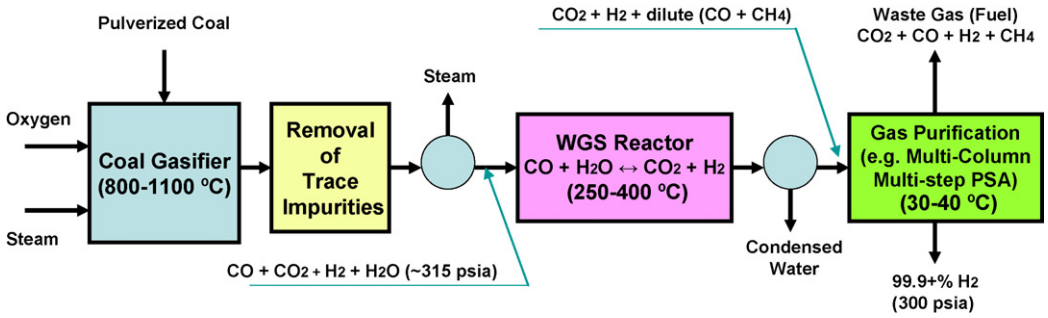

Fig. 1. Flow sheet for conventional route of H_2 production by coal gasification.

rinse step, and a high pressure, high temperature steam purge step.

Fig. 1 shows the conventional flow diagram for production of H_2 by coal gasification using a WGS reactor and a multi-column, multi-step pressure swing adsorption (PSA) unit which produces a fuel-cell grade H_2 product gas with or without any by-product CO_2 recovery [3–6]. The H_2 is produced at the feed gas pressure while the CO_2 by-product gas (optional) is produced at near ambient pressure. A part (~10–25%) of the product H_2 by the PSA process is used as the purge gas for periodic regeneration of the CO_2 physi-sorbent used in the process. This H_2 is lost and combusted as fuel.

Fig. 2 is a schematic representation of the proposed TSSER concept showing that a single sorber-reactor replaces the complex WGS–PSA units of the conventional process while simultaneously producing a pure H_2 product gas at reactor feed pressure and a compressed by-product CO_2 gas.

The proposed TSSER process concept offers the following key advantages [2]:

- Removal of CO_2 from the reaction zone of the WGS reactor drives the WGS reaction forward according to the Le Chatelier's principle. This permits (i) higher conversion of CO to H_2 than that governed by the thermodynamic equilibrium, (ii) enhancement of the forward reaction rate, (iii) the use of a lower H_2O/CO ratio in the feed gas, and (iv) relatively higher temperature operation of the reactor without the thermodynamic penalty.
- The concept permits direct production of CO_x-free H_2 from the reactor at feed gas pressure, which eliminates requirement for a subsequent separation process.
- Simultaneous production of an essentially pure and compressed CO_2 by-product facilitates (i) subsequent CO_2 sequestration (elimination of green house gas emission) or (ii) sale of CO_2 by-product.
- Use of extraneous super-heated steam as the regeneration gas for the CO_2 chemisorbent in the TSSER process permits significantly larger net H_2 recovery by the process compared to the conventional process where the PSA H_2 purification system typically loses 10–25% of product H_2 as the purge gas.
- Potential for significant savings in capital and energy costs due to simpler equipment, absence of high temperature metallurgical demands, elimination of separate product purification unit, and a small footprint of the overall process.

The cyclic TSSER process consists of five sequential steps. They include (a) sorption-enhanced reaction step, (b) high pressure CO_2 rinse step, (c) batch heating step, (d) high pressure steam purge step, and (e) multi-tasking regeneration step consisting of sub-steps like depressurization, cooling, low pressure steam purge and pressurization. Fig. 3 represents a schematic description of these steps. A more detailed description of the operation of each step can be found elsewhere [2].

The key functions of the individual steps of the proposed TSSER process are as follows:

- Step (a) achieves nearly complete conversion of CO to H_2 and produces fuel-cell grade H_2 (dry basis) at reactor pressure by circumventing the thermodynamic limitation of the reversible WGS reaction.

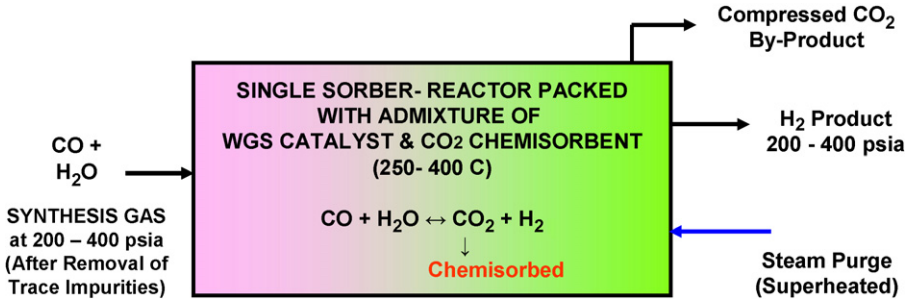

Fig. 2. Schematic concept of TSSER process.

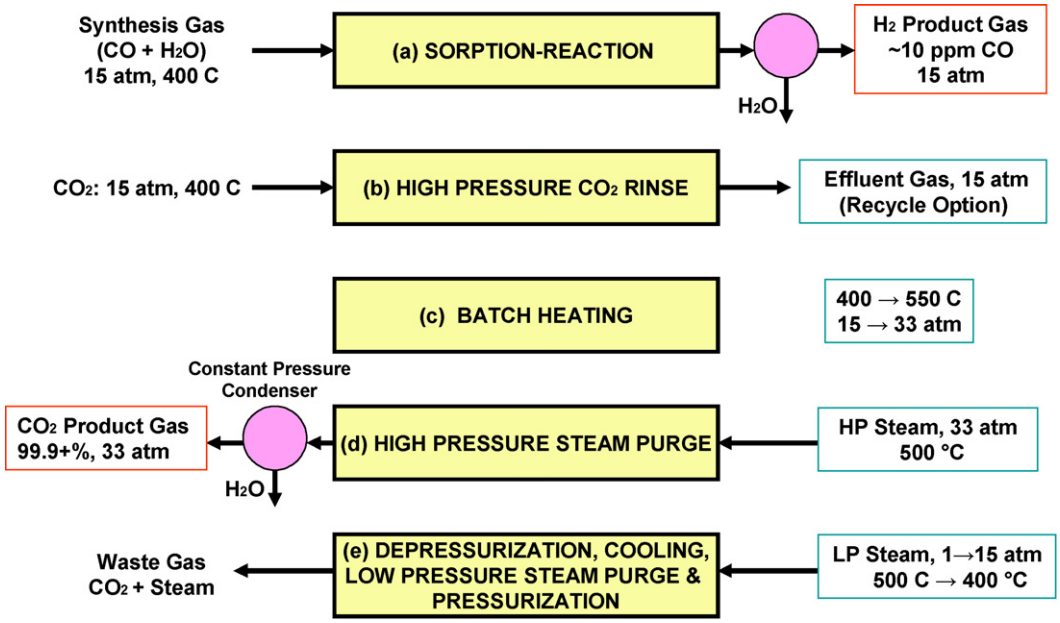

Fig. 3. Schematic representation of the TSSER process steps (time (min) for steps: (a) 10, (b) 1, (c) 10, (d) 10, and (e) 9), HP = high pressure and LP = low pressure.

- Step (b) replaces the sorber-reactor void gas with pure CO_2 at reactor pressure and facilitates production of pure CO_2 by-product in step (d).
- Step (c) compresses the gas inside the sorber-reactor above the feed gas pressure by thermal desorption of CO_2 and produces compressed, by-product CO_2 in step (d).
- Step (d) produces compressed high purity CO_2 by-product (dry basis) gas while partially regenerating the chemisorbent.
- Step (e) provides the final regeneration of the sorbent and prepares the sorber-reactor to begin a new cycle.

The combined effects of these steps of the process are: (i) very high cyclic CO_2 working capacity, (ii) low net steam consumption for regeneration, and (iii) compact and small footprint process design.

The process performance of the TSSER concept was recently simulated using an ideal synthesis gas containing a binary mixture of CO and H_2O ($CO:H_2O = 1:4$, pressure = 15 atm, and temperature = 400 °C) as the feed gas to the sorber-reactor in step (a) of the cycle. The tube and shell reactor was packed with an admixture of 10% WGS catalyst and 90% CO_2 chemisorbent (by weight). A novel CO_2 chemisorbent, K_2CO_3 promoted hydrotalcite, which was extensively characterized by measuring its CO_2 sorption capacities at different temperatures and its CO_2 ad(de)sorption column dynamics at different temperatures was used as the CO_2 chemisorbent [7]. The material selectively and reversibly chemisorbs CO_2 from mixtures with CO, H_2, CH_4 and H_2O in the temperature range of 350–500 °C with good capacity and fast kinetics. A new chemisorption equilibrium model invoking simultaneous surface chemisorption of CO_2 and additional complexation reaction between gaseous and chemisorbed CO_2 molecules was used to describe the experimental CO_2 chemisorption isotherms [7], and a conventional linear driving force (LDF) model was used for describing CO_2 chemisorption kinetics [8]. The kinetics of the WGS reaction was described by an empirical model [9]. A mathematical framework based on the well-known "continuous stirred tank reactor (CSTR) in series" model was used to simulate each individual step of the process. The key assumptions and the methods of solution of the simultaneous mass and energy balance equations of the process model can be found elsewhere [10]. The shell side of the reactor was maintained at 400 °C during steps (a), (b), and (e) and at 550 °C during steps (c) and (d) of the process. Pure CO_2 was co-currently introduced into the reactor tube at 15 atm and 400 °C during step (b). Super-heated steam was counter-currently introduced into the reactor tube at 550 °C during step (d) and at 400 °C during step (e). The steam pressures were equal to the prevailing sorber-reactor pressures [2]. The previously simulated performance of the TSSER process using the promoted hydrotalcite as the CO_2 chemisorbent is reproduced in the second column of Table 4 [2]. The process is capable of simultaneously producing fuel-cell grade H_2 and compressed CO_2 by-product from a synthesis gas feed. The H_2 productivity by the process (both moles of H_2 produced/mole of CO in feed gas and moles of H_2 produced/kg of total solid in sorber-reactor/cycle) is high. The by-product CO_2 is nearly pure and it is compressed to a pressure of ~33 atm by the process. Nearly 60% of the CO_2 produced by the WGS reaction is recovered as the by-product.

The objective of this work is to report the simulated performance of the above-described TSSER process using another reversible CO_2 selective chemisorbent, Na_2O promoted alumina, which was developed for removal of CO_2 from a hot and wet waste gas [11]. Extensive equilibrium and column dynamic characteristics for chemisorption of CO_2 on this material were recently measured in the temperature range of 250–450 °C [12]. They are summarized below.

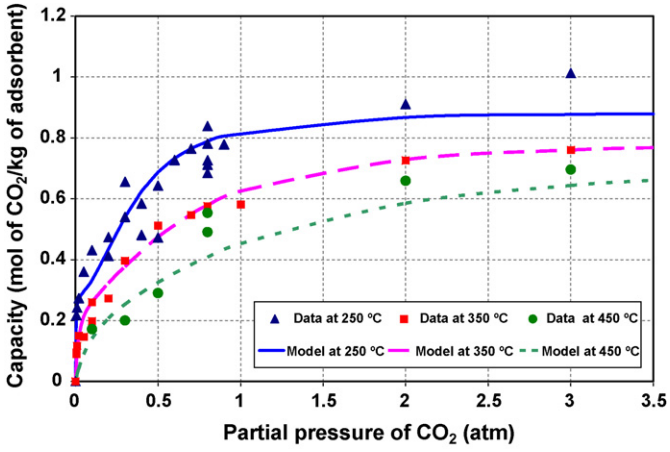

Fig. 4. CO_2 chemisorption isotherms on Na_2O promoted alumina.

2. CO_2 chemisorption equilibria on promoted alumina

Fig. 4 shows the experimentally measured CO_2 sorption isotherms on the promoted alumina at 250, 350 and 450 °C in the pressure range of 0–3 atm. The isotherms were measured by analyzing the CO_2 column breakthrough data using different mixtures of CO_2 and N_2 as the feed gas. More details of the experimental procedure and data analysis can be found elsewhere [12].

The figure also shows the best fit of the CO_2 chemisorption isotherms using a newly proposed chemisorption equilibrium model invoking simultaneous chemisorption–surface complexation which leads to the following analytical equation [7]:

$$n^*(P,T) = \frac{mK_CP[1+(a+1)K_RP^a]}{1+K_CP+K_CK_RP^{(a+1)}} \quad (1)$$

where n^* is the specific equilibrium amount (mol kg^{-1}) of CO_2 chemisorbed on the promoted alumina at pressure P (atm) and temperature T (K). The parameters of model equation (1) are the saturation CO_2 chemisorption capacity of the chemisorbent surface, m (mol kg^{-1}), the equilibrium constant for surface chemisorption of CO_2, K_C (atm^{-1}), the equilibrium constant for the additional complexation reaction between the gaseous and chemisorbed molecules of CO_2, K_R (atm^{-a}), and the stoichiometric coefficient for the complexation reaction, a. The thermodynamic constants (K_C and K_R) are exponential functions of temperature:

$$\frac{d\ln K_C}{dT} = -\frac{q_C}{RT^2} \qquad \frac{d\ln K_R}{dT} = -\frac{\Delta H_R}{RT^2} \quad (2)$$

$$K_C = K_C^0 \exp\left[\frac{q_C}{RT}\right] \qquad K_R = K_R^0 \exp\left[\frac{\Delta H_R}{RT}\right] \quad (3)$$

where q_C and ΔH_R (kJ mol^{-1}) are, respectively, the molar isosteric heat of chemisorption and the heat of additional surface reaction. K_C^0 (atm^{-1}) and K_R^0 (atm^{-a}) are constants.

It can be shown that (i) Eq. (1) has the same form as the Langmuir isotherm model (Eq. (4)) in the low pressure region, and (ii) n^* asymptotically approaches a saturation capacity $[n^m = m(a+1)]$ at the limit of $P \to \infty$:

$$n^*(P,T) = \frac{mK_CP}{[1+K_CP]} \quad \text{for small values of } P \text{ or } n^* \quad (4)$$

The solid and dashed lines of Fig. 4 show the fit of the experimental chemisorption isotherms of CO_2 on Na_2O promoted alumina at 250, 350 and 450 °C by Eq. (1). The model parameters are given in Table 1. It also gives the Henry's law constants ($K_H = mK_C$) at different temperatures.

It may be seen from Fig. 4 that the new model describes the experimental chemisorption isotherm data fairly well. The heats of chemisorption and the surface reaction were estimated to be, respectively, 64.9 and 37.5 kJ mol^{-1}.

The corresponding pre-exponential constants (Eq. (3)) were, respectively, 0.000164 (atm^{-1}) and 0.001417 atm^{-a}. The parameter 'a' was an exponential function of temperature:

$$a = 0.72644 \exp\left[\frac{4.39\ \text{kJ mol}^{-1}}{RT}\right] \quad (5)$$

3. CO_2 chemisorption kinetics on promoted alumina

The kinetics of chemisorption of CO_2 on the promoted alumina were evaluated by analyzing (i) the column breakthrough data for adsorption of CO_2 from different mixtures with inert N_2 and (ii) the desorption characteristics of 40% $CO_2 + N_2$ from a column by inert N_2 purge [12]. A linear driving force (LDF) model was used to extract the effective mass transfer coefficients for ad(de)sorption of CO_2 on the material from these data [8]:

$$\text{LDF model}: \quad \frac{dn(t)}{dt} = k[n^*(t) - n(t)] \quad (6)$$

Eq. (6) gives the local rate of ad(de)sorption of CO_2 from an inert gas inside the column. $n(t)$ is the specific amount (mol kg^{-1}) of CO_2 chemisorbed at time t and $n^*(t)$ is the specific equilibrium adsorption capacity of CO_2 at the prevailing gas phase at pressure P_0, temperature $T(t)$ and CO_2 mole fraction of $y(t)$. n^* is given by Eq. (1) for a given set of P_0, y, and T. The parameter k (time^{-1}) is the LDF mass transfer coefficient for CO_2 ad(de)sorption.

Fig. 5 shows examples of the column breakthrough data (effluent gas concentration (y) as a function of dimensionless

Table 1
Parameters of chemisorption–surface reaction model for sorption of CO_2 on Na_2O promoted alumina

T (°C)	m (mol kg^{-1})	a	K_C (atm^{-1})	K_R (atm^{-a})	$K_H = mK_C$ (mol (kg atm)$^{-1}$)
250	0.295	2.0	536	8	158
350	0.295	1.7	48.3	2	14.2
450	0.295	1.5	8.47	0.73	2.45

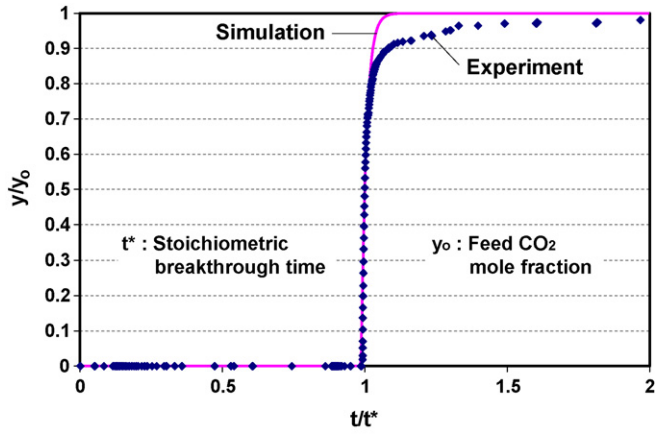

Fig. 5. Column breakthrough data for sorption of 60% CO_2 from N_2 at 350 °C.

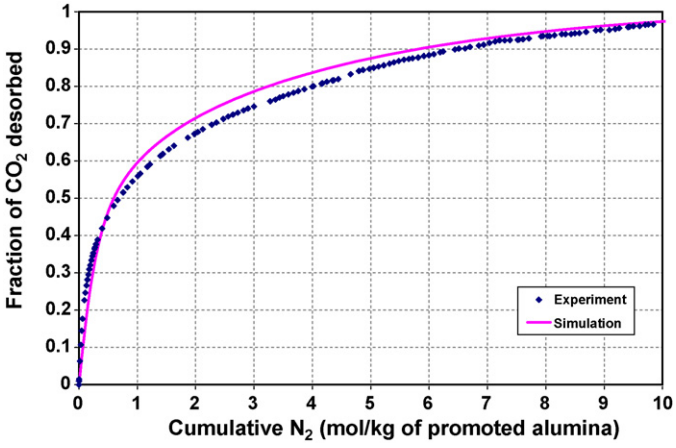

Fig. 6. CO_2 desorption characteristics from promoted alumina at 350 °C.

time) for adsorption of 60% CO_2 (y_0) from N_2 on the promoted alumina. Fig. 6 shows the column dynamic data (fraction of CO_2 desorbed as a function of inlet N_2 purge gas quantity) for desorption of 40% $CO_2 + N_2$ by N_2 purge at 350 °C and a total gas pressure of ~1 atm. The length of the packed column (diameter = 1.73 cm) was 97.3 cm. The solid lines in Figs. 5 and 6 show the corresponding CO_2 adsorption and desorption characteristics simulated by the "CSTR in series" model and the CO_2 adsorption equilibrium and kinetic parameters of Tables 1 and 2. More detailed description of the experimental procedure and data analysis can be found elsewhere [12].

The CO_2 mass transfer coefficients on the promoted alumina were found to be independent of CO_2 concentrations in the range of test data ($0.4 \leq y_0 \leq 0.6$) for a given temperature, and they were identical for both adsorption and desorption of CO_2. The coefficients were rather a weak function of temperature as given in Table 2.

Table 2
LDF mass transfer coefficients for ad(de)sorption of CO_2 on promoted alumina

Temperature (°C)	k (min^{-1})
250	4.0
350	5.0

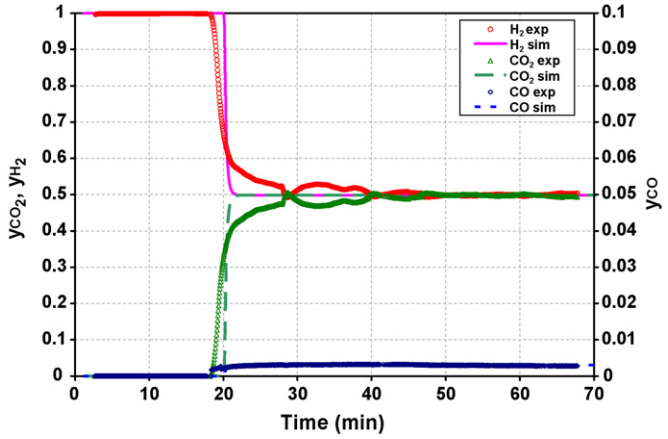

Fig. 7. Transient effluent gas compositions from SER reactor.

4. Demonstration of sorption-enhanced reaction (SER) concept

The concept of sorption-enhanced reaction for WGS reaction was experimentally demonstrated by packing a tubular reactor (1.73 cm diameter × 86.4 cm long) with an admixture of a commercial WGS catalyst ($Cu/ZnO/Al_2O_3$ LTS catalyst produced by Sud Chemie of Switzerland) and the above-mentioned CO_2 chemisorbent (promoted alumina). The ratio of chemisorbent/catalyst was 70:30 (wt.%). The reactor was heated to and maintained at a temperature of 300 °C using heating tapes. It was initially filled with a gas mixture containing argon (36.7%) and steam (63.3%) at 1 atm. A gaseous mixture consisting of 10.9% CO, 56.4% H_2O and 32.7% Ar at ambient pressure and 300 °C was passed through the reactor. The total gas flow rate was 458.6 cm^3 min^{-1}. The composition of the effluent gas was continuously analyzed using a quadrupole mass spectrometer. Fig. 7 shows the transient reactor effluent gas compositions of H_2, CO_2, and CO in a dry and argon free basis. These experiments were repeated four times to check reproducibility.

It may be seen from Fig. 7 that CO_x-free H_2 is produced from the reactor by reaction between CO and H_2O (WGS reaction) for a period of time. This is caused by simultaneous removal of CO_2 from the reaction zone by chemisorption on the promoted alumina, which circumvents the thermodynamic limitation of the WGS reaction and produces a pure H_2 product gas. This sorption-enhanced reaction process continues until the CO_2 chemisorption capacity of the promoted alumina is exhausted. Thereafter, the H_2 concentration in the effluent gas rapidly falls and the CO and CO_2 concentrations rapidly rise to a composition (49.85% H_2 + 49.85% CO_2 + 0.3% CO on dry and argon free basis) which is dictated by the thermodynamics of the WGS reaction at the conditions of the test (feed gas composition and reactor temperature). Fig. 7, therefore, is an experimental demonstration of the SER concept for WGS reaction carried out in presence of Na_2O promoted alumina as a CO_2 chemisorbent. The solid and dashed lines in Fig. 7 represent the reactor effluent gas composition profiles for the conditions of the experiment simulated by the "CSTR in series" model using the CO_2 sorption characteristics of promoted alumina reported in this work

and a published empirical model of the WGS reaction kinetics [10,13]. It may be seen that the simulated reactor effluent gas profiles trace the experimental profiles fairly well indicating the validity of the model for this application. The stoichiometric time for the breakthrough of CO_x from the sorber-reactor under the conditions of the experiments was 20.2 min.

5. Comparative CO_2 chemisorption characteristics of Na_2O promoted alumina and K_2CO_3 promoted hydrotalcite

Table 3 compares some of the key equilibrium parameters of the CO_2 chemisorption–surface complexation model and the LDF kinetic parameter on Na_2O promoted alumina and K_2CO_3 promoted hydrotalcite [7,12]:

Table 3 shows that the isosteric heat of chemisorption (q_C) of CO_2 on the promoted alumina is ~3 times larger than that on the promoted hydrotalcite. On the other hand, the heats of surface complexation reaction (ΔH_R) are comparable for both chemisorbents. The Henry's law constant for the chemisorption isotherm at 400 °C on the promoted alumina is only about half of that for the promoted hydrotalcite. The LDF mass transfer coefficients (k) for chemisorption of CO_2 on these materials have the same order of magnitude, the coefficient for promoted alumina being larger than that on the promoted hydrotalcite. The cause for the differences in the heats of chemisorption of CO_2 on these two materials is presently unknown. A detailed analysis of the chemical structure of the chemisorbed and surface complexation species will be necessary to explain this behavior. Nevertheless, these heats cause a very significant difference in the overall shapes of the CO_2 chemisorption isotherms on these materials as functions of temperature. Fig. 8 shows the CO_2 isotherms at 400 and 550 °C on these materials calculated by Eq. (1).

Several very interesting differences in the shapes of the CO_2 isotherms on these chemisorbents are:

- The temperature coefficients of the CO_2 sorption capacities in the low CO_2 pressure region are much less pronounced on the promoted hydrotalcite than on the promoted alumina due to much higher isosteric heat of adsorption of the CO_2 on the promoted alumina.
- The inflection in the CO_2 isotherm shape at 400 °C is more pronounced for the promoted hydrotalcite.
- The CO_2 sorption capacity on the promoted alumina at 550 °C and any given pressure is much lower than that on the promoted hydrotalcite, particularly in the low-pressure region.

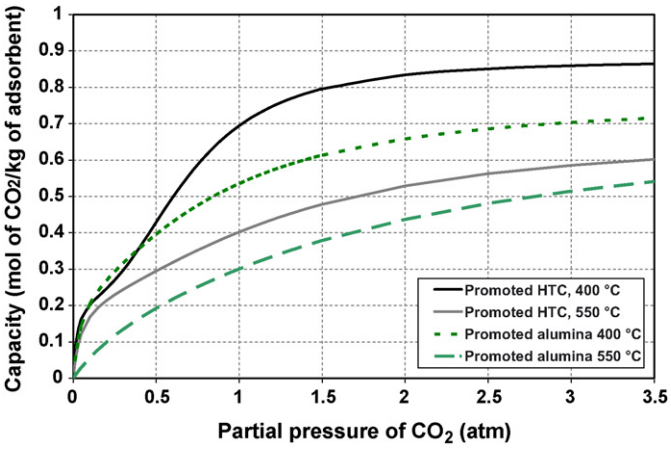

Fig. 8. Comparison of CO_2 isotherms on the chemisorbents at 400 and 550 °C.

- The CO_2 sorption capacities at 400 °C are comparable on both materials despite their different shapes in the low-pressure region ($P_{CO_2} < 0.5$ atm). The CO_2 capacity on the promoted hydrotalcite is larger than that on the alumina at the high-pressure region.
- The Henry's law constant for CO_2 sorption on the promoted alumina at 550 °C is significantly lower than that for the promoted hydrotalcite.

6. Comparative TSSER process performance

The net effects of the differences in the shapes of the CO_2 chemisorption isotherms of the chemisorbents on the performance of the above-described, five-step TSSER process cannot be predicted a priori without simulating the process performance. However, the lower Henry's law constant for the CO_2 isotherm on the promoted alumina at 400 and 550 °C will facilitate its desorption by steam purge (process steps (d) and (e)).

Table 4 compares the simulated performance of the TSSER process using the chemisorbents. The conditions of operation of the process were given earlier. The only difference was in the gas flow rates for the different steps of the process as summarized in Table 5. The process performance of the promoted hydrotalcite was published earlier [2]. The corresponding process performance of the promoted alumina is new. The sorber-reactor was nearly completely regenerated (~98.2% CO_2 removed per cycle) for both chemisorbents.

Table 4 shows that the promoted alumina is also capable of simultaneously producing fuel-cell grade H_2 and compressed CO_2 by-product gas from the synthesis gas feed. The key performance differences for using the promoted alumina

Table 3
Comparative equilibrium and kinetic characteristics for chemisorption of CO_2

Chemisorbent	Heat of CO_2 chemisorption, q_c (kJ mol^{-1})	Heat of additional CO_2 complexation reaction, ΔH_R (kJ mol^{-1})	Henry's law constant, K_H (mol (kg atm)$^{-1}$)		LDF kinetic parameter, k (min^{-1})
			400 °C	550 °C	
Promoted alumina	64.9	37.5	5.6	0.67	5.0 at 350 °C
Promoted hydrotalcite	21.0	42.2	9.4	4.7	3.0 at 400 °C

Table 4
Comparison of performance and productivity of TSSER-WGS processes for different chemisorbents (feed: 1:4 $CO + H_2O$ at 400 °C and 15 atm)

Chemisorbent	Promoted hydrotalcite	Promoted alumina
Moles (net) of H_2 product per mole of CO in feed gas	0.933	0.915
High purity H_2 produced per cycle (~10 ppm CO, 15 atm)	0.710 mol kg^{-1} of solid	0.601 mol kg^{-1} of solid
Pure CO_2 produced at high pressure (~100% CO_2)	0.761 mol kg^{-1} of solid (33.1 atm)	0.789 mol kg^{-1} of solid (22.6 atm)
Net amount of CO_2 produced (~100% CO_2)	0.433 mol kg^{-1} of solid (33.1 atm)	0.416 mol kg^{-1} of solid (22.6 atm)
Net CO_2 recovery as compressed by-product gas (%)	57.1	63.4
CO_2 removed from bed	74.2% (step (d)), 98.2% (step (d) + step (e))	84.4% (step (d)), 98.2% (step (d) + step (e))
Steam duty (steps (d) + (e))	7.84 mol kg^{-1} of solid = 0.262 tons/MSCF H_2	4.19 mol kg^{-1} of solid = 0.159 tons/MSCF H_2
Cost of steam purge (steps (d) + (e))	\$0.66* of steam/MSCF H_2 (*\$2.5 (ton steam)$^{-1}$)	\$0.40* of steam/MSCF H_2 (*\$2.5 (ton steam)$^{-1}$)

Table 5
Inlet gas flow rates for different steps of the simulated TSSER process

Chemisorbent	Inlet gas flow rates (mol (cm^2 min)$^{-1}$)			
	Step (a)	Step (b)	Step (d)	Step (e)
Promoted hydrotalcite	0.157	0.135	0.157	0.157
Promoted alumina	0.115	0.130	0.115	0.011

instead of the promoted hydrotalcite as the CO_2 chemisorbent are:

- 15% reduction in the productivity (mol kg^{-1} of solid/cycle) of fuel-cell grade H_2 at nearly equal net conversion of CO to H_2.
- 4% reduction in the productivity (mol kg^{-1} of solid/cycle) of compressed by-product CO_2.
- 6% points increase in the recovery of product CO_2.
- Lesser but still significant compression of the CO_2 by-product.
- 50% reduction in the net steam duty [tons/thousand standard cubic feet (MSCF) H_2] for regeneration of the chemisorbent.

This last issue may be important because it substantially reduces the cost of steam utility for the TSSER process. A detailed economic evaluation of the performances of the two materials, however, will be necessary to establish the relative merits of the above-listed pros and cons. That was not a goal of this work.

Fig. 9 compares the simulated CO_2 desorption characteristics for the TSSER process (steps (d) and (e)) using steam purge for the two chemisorbents. It plots the fraction of CO_2 removed as a function of cumulative amount of steam purge for steps (d) and (e) of the process. The fractional amounts of CO_2 removed by steps (d) and (e) of the process using these chemisorbents are different. However, the fractional amounts of CO_2 removed per cycle of the process are identical for both chemisorbents. The shapes of the CO_2 desorption characteristics of Fig. 9 are directly influenced by the shapes of the isotherms in Fig. 8. In particular, the very efficient desorption of CO_2 during step (e) of the TSSER process using the promoted alumina is caused by its lower Henry's law constant.

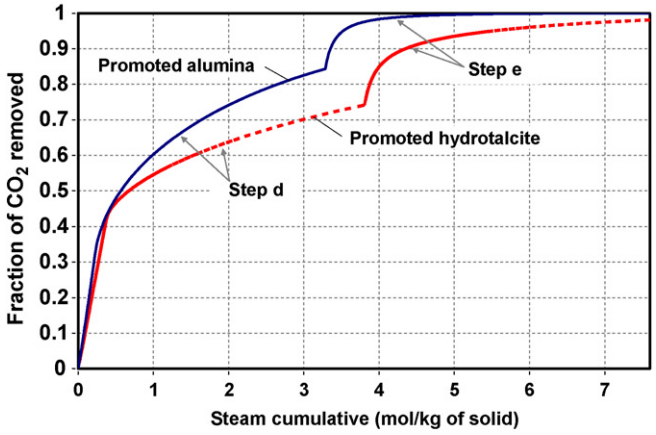

Fig. 9. Comparative desorption of CO_2 for the chemisorbents by the TSSER process.

7. Summary

The simulated process performance of a novel five-step thermal swing sorption-enhanced reaction (TSSER) process concept, which directly and simultaneously produces fuel-cell grade (~10 ppm CO) H_2 and pure (~99.9+%) compressed CO_2 from a synthesis gas ($CO + H_2O$) feed, is described. Na_2O promoted alumina is used as a CO_2 selective chemisorbent in the process. The concept simultaneously carries out the reversible water gas shift (WGS) reaction and chemisorption of CO_2 from the reaction zone in a single unit operation. New experimental data is reported to demonstrate the sorption-enhanced reaction concept for WGS reaction.

The H_2 is produced at the feed gas pressure, and the CO_2 by-product is compressed by the process much above the feed gas pressure. The process offers very high conversion of CO to H_2 and high utilization of the CO_2 sorption capacity of the chemisorbent. The periodic regeneration of the chemisorbent is achieved by a two-stage super-heated steam purge.

A comparison between the performances of Na_2O promoted alumina and K_2CO_3 promoted hydrotalcite as the CO_2 selective chemisorbent in the TSSER process using a feed gas containing 1:4 $CO:H_2O$ at 15 atm and 400 °C indicates that about 50% reduction in the steam requirement for the regeneration of the

chemisorbent can be achieved by using the promoted alumina. This is accompanied by about 15% reduction in the H_2 productivity and about 6% gain in the recovery of the by-product CO_2. The pressures of the by-product CO_2 gas are, respectively, 22.6 and 33.1 atm for the promoted alumina and the promoted hydrotalcite cases. These process performances are primarily governed by the shapes of the chemisorption isotherms at different temperatures and the heats of CO_2 chemisorption and surface complexation reactions for the chemisorbents.

Acknowledgements

The work was partly supported by the Pennsylvania Infrastructure Technology Alliance grants (PITA-442-04 and PITA-542-5), by the U.S. Department of Energy under cooperative agreement DE-P S26-04NT-42454, and by a donation from Air Products and Chemicals Inc.

References

[1] National Research Council and National Academy of Engineering, The Hydrogen Economy: Opportunities, Costs, Barriers, and R&D Needs, The National Academy Press, Washington, DC, 2004.
[2] K.B. Lee, M.G. Beaver, H.S. Caram, S. Sircar, Reversible chemisorption of carbon dioxide: simultaneous production of fuel-cell grade H_2 and compressed CO_2 from synthesis gas, Adsorption 13 (2007) 385–397.
[3] A. Fuderer, Selective adsorption process for production of ammonia synthesis gas mixtures, US Patent 4,375,363 (1983).
[4] S. Sircar, T.C. Golden, Sep. Sci. Technol. 35 (2000) 667–687.
[5] S. Sircar, Separation of multi-component gas mixtures, U.S. Patent 4,077,779 (1979).
[6] S. Sircar, W.C. Kratz, Sep. Sci. Technol. 23 (1988) 2397–2415.
[7] K.B. Lee, A. Verdooren, H.S. Caram, S. Sircar, J. Colloid Interf. Sci. 308 (2007) 30–39.
[8] S. Sircar, J.R. Hufton, Adsorption 6 (2000) 137–147.
[9] J.G. Xu, G.F. Froment, AIChE J. 35 (1989) 88–96.
[10] K.B. Lee, M.G. Beaver, H.S. Caram, S. Sircar, Ind. Eng. Chem. Res. 41 (2007) 5003–5014.
[11] S. Sircar, C.M.A. Golden, PSA process for removal of bulk CO_2 from a wet high temperature gas, U.S. Patent 6,322,612 (2001).
[12] K.B. Lee, M.G. Beaver, H.S. Caram, S. Sircar, AIChE J. 53 (2007) 2824–2831.
[13] Y. Choi, H.G. Stenger, J. Power Sources 124 (2003) 432–439.